The Astrophysical Journal Supplement Series, 226:21 (6pp), 2016 October doi:10.3847/0067-0049/226/2/21

A CATALOG OF ECLIPSING BINARIES AND VARIABLE STARS OBSERVED WITH ASTEP 400 FROM DOME C, ANTARCTICA

E. Chapellier[1], D. Mékarnia[1], L. Abe[1], T. Guillot[1], K. Agabi[1], J.-P. Rivet[1], F.-X. Schmider[1], N. Crouzet[2], and E. Aristidi[1]
[1] Laboratoire Lagrange, Université Côte d'Azur, Observatoire de la Côte d'Azur, CNRS, Boulevard de l'Observatoire, CS 34229, F-06304 Nice Cedex 4, France
[2] Dunlap Institute for Astronomy & Astrophysics, University of Toronto, 50 St. George Street, Toronto, ON M5S 3H4, Canada
Received 2016 July 4; revised 2016 September 1; accepted 2016 September 6; published 2016 October 17

ABSTRACT

We used the large photometric database of the ASTEP program, whose primary goal was to detect exoplanets in the southern hemisphere from Antarctica, to search for eclipsing binaries (EcBs) and variable stars. 673 EcBs and 1166 variable stars were detected, including 31 previously known stars. The resulting online catalogs give the identification, the classification, the period, and the depth or semi-amplitude of each star. Data and light curves for each object are available at http://astep-vo.oca.eu.

Key words: catalogs – binaries: eclipsing – stars: variables: delta Scuti – stars: variables: general – stars: variables: RR Lyrae – techniques: photometric

Supporting material: machine-readable tables

1. INTRODUCTION

The space missions *MOST* (Walker et al. 2003), CoRot (Baglin et al. 2006), and *Kepler* (Borucki et al. 2010) have shown the advantages of long-term continuous monitoring of large samples of stars. Significant amounts of exoplanets, eclipsing binaries (EcBs), and variable stars have been detected and analyzed, leading to many high-impact discoveries. Even if space is, of course, the best place to acquire such high-quality data, the long polar winter nights in Antarctica also permit the accumulation of quasi-continuous observations with good quality.

ASTEP 400 is a semi-robotic and fully computer-controlled telescope built to withstand the harsh conditions in Antarctica and to perform high-precision photometry (Daban et al. 2010; Abe et al. 2013; Mékarnia et al. 2016). These specifications make this instrument ideal for monitoring several thousands of stars to search for transiting exoplanets, and well-suited for a variety of wide field imaging and temporal studies, such as the discovery and monitoring of EcBs and variable stars. ASTEP 400 used facilities provided by the French–Italian Antarctic station Concordia, located at Dome C (75°06′S, 123°21′E) in Antarctica at an altitude of 3233 m.

In this paper we present our catalogs of EcBs and variable stars detected by ASTEP 400 during the 2010−2012 Antarctic winter seasons. Section 2 presents the description of the telescope, the observations, the processing of data, and the selection and classification methods used. Catalogs of the detected EcBs and variable stars are presented in Sections 3 and 4. Finally, the summary and conclusions of this paper can be found in Section 5.

2. OBSERVATIONS AND DATA REDUCTION

Observations were carried out using the ASTEP 400 telescope, described in detail in Mékarnia et al. (2016). Briefly, ASTEP 400 is a custom 40 cm Newtonian telescope equipped with a 5-lens Wynne coma corrector and a 4k × 4k front-illuminated FLI Proline KAF 16801E CCD. The corresponding field of view (FOV) is $1^\circ \times 1^\circ$, with a plate scale of 0.93 arcsec pixel^{-1}. The telescope is also equipped with a SBIG ST402M guiding camera, which ensures, in normal observing conditions, a guiding stability of about 0.2 arcsec rms or better. A dichroic plate is used to separate the "science" path from the telescope "guiding" path. The red part of the spectrum ($\lambda > 0.6\ \mu$m) is sent to the "science" camera, while the blue part ($\lambda < 0.6\ \mu$m) is directed to the guiding camera. No filter is used and most of the "science" signal is transmitted in the red part.

Scientific ASTEP 400 observations were conducted from 2010 to 2012, between the beginning of March through the end of September of each polar campaign. For each selected field, acquisition was performed automatically, when the Sun elevation was lower than -9°. If we compare the effective observation time to the spell of dark nights (i.e., when the Sun is 9° below the horizon) the average duty cycle is equal to 65.14%.

Table 1 lists the coordinates, the exposure time, the observation period, the number of frames, and the available observation time of each observed stellar field. More than 150,000 images were collected for a total integration time of 3729 hr.

The ASTEP 400 data reduction pipeline, only briefly described here (see Abe et al. 2013 for a complete description), involves bias and dark subtraction, flat-fielding, bad-pixel-masking, and optimal image subtraction (OIS) photometry (Miller et al. 2008), including correction of the nonlinearity of the CCD. Flat-fielding over a wide FOV, as done for ASTEP 400, is affected by the sky-concentration effect, which causes an additive bell-shaped halo component to be present in the center of each frame (Andersen et al. 1995). We used satellite trails to remove this effect for both image and flat-field frames (Abe et al. 2013).

Figure 1 shows a typical photometric precision obtained by ASTEP 400. The rms noise varies from ∼2 parts per thousand (ppt) for the brightest stars ($R \sim 12$ mag), with an integration time of 130 s, to ∼20 ppt for the faintest stars ($R = 17.5$ mag). Stars brighter than $R \sim 11.5$ mag were excluded because of detector saturation.

Since the main goal of ASTEP 400 was to find and characterize transiting exoplanets, a box-fitting algorithm (BLS: Box-fitting Least Squares; Kovács et al. 2002) was applied to the calibrated light curves to search for planetary

Table 1
Observation Information of the ASTEP Fields

Field	Coordinates (J2000.0) α	Coordinates (J2000.0) δ	Exp. Time (s)	Date of Observation Start	Date of Observation End	Frames	Total Exp. Time (hr)
F-01	$09^{h}53^{m}56^{s}.00$	$-45°46'13''.50$	130	2010 Apr 30	2010 May 24	8067	336.12
F-02	$15^{h}56^{m}18^{s}.70$	$-66°25'24''.70$	120	2010 May 26	2010 Jun 07	5891	229.09
	…	…	70	2010 Aug 02	2010 Aug 08	1845	46.12
F-03	$15^{h}54^{m}48^{s}.40$	$-65°54'04''.30$	70	2010 Jul 15	2010 Aug 02	7864	196.60
	…	…	100	2012 Aug 31	2012 Sep 28	3622	120.73
F-04	$15^{h}46^{m}11^{s}.00$	$-64°53'32''.59$	70	2010 Jul 24	2010 Aug 08	5396	134.90
F-05	$15^{h}43^{m}50^{s}.79$	$-66°31'13''.89$	70	2010 Sep 17	2010 Sep 23	898	22.45
F-06	$16^{h}10^{m}51^{s}.29$	$-66°21'25''.10$	70	2010 Sep 17	2010 Sep 26	3175	79.37
	…	…	30	2011 Mar 29	2011 Apr 23	14490	201.25
	…	…	60	2011 Aug 12	2011 Aug 29	7272	193.00
F-07	$17^{h}16^{m}32^{s}.70$	$-55°30'04''.59$	60	2011 Apr 26	2011 May 14	5295	191.22
F-08	$17^{h}35^{m}29^{s}.10$	$-55°45'47''.09$	60	2011 May 14	2011 May 31	10957	243.49
F-09	$17^{h}36^{m}16^{s}.00$	$-53°48'43''.09$	60	2011 May 31	2011 Jun 09	7699	171.09
	…	…	60	2011 Aug 30	2011 Sep 13	4936	139.52
F-10	$17^{h}20^{m}37^{s}.00$	$-59°26'25''.79$	60	2011 Jun 10	2011 Jun 20	9443	209.84
F-11	$17^{h}44^{m}57^{s}.59$	$-58°21'16''.60$	60	2011 Jun 21	2011 Jun 29	8495	198.78
F-12	$17^{h}35^{m}19^{s}.89$	$-53°21'10''.39$	60	2011 Jun 30	2011 Jul 14	9443	209.84
F-13	$17^{h}48^{m}03^{s}.40$	$-59°26'52''.50$	60	2011 Jul 15	2011 Jul 28	9781	217.35
F-14	$17^{h}35^{m}25^{s}.00$	$-57°51'23''.10$	60	2011 Jul 29	2011 Aug 11	7556	167.91
F-15	$17^{h}21^{m}51^{s}.00$	$-53°00'22''.10$	60	2012 Apr 12	2012 Apr 26	6928	153.96
F-16	$17^{h}12^{m}14^{s}.10$	$-52°17'54''.90$	60	2012 Apr 27	2012 May 07	6805	151.22
F-17	$17^{h}07^{m}31^{s}.39$	$-48°14'53''.90$	40	2012 May 11	2012 May 13	2210	36.83
F-18	$16^{h}23^{m}09^{s}.30$	$-48°38'26''.20$	90	2012 May 26	2012 Jun 02	2563	78.32

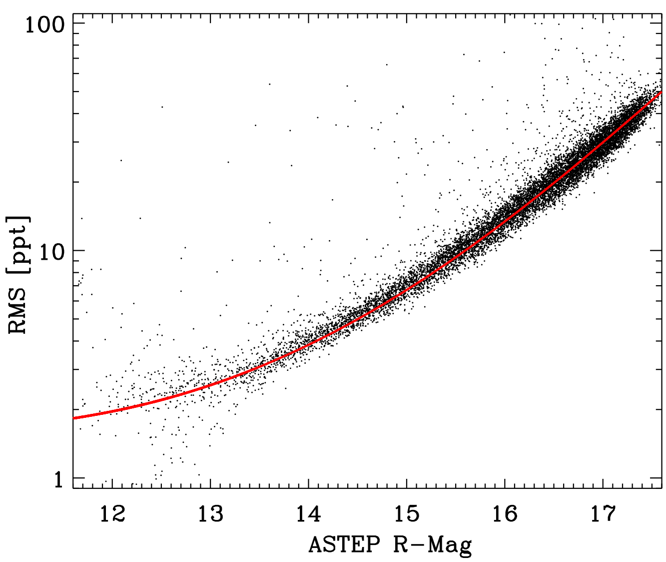

Figure 1. Typical photometric precision obtained with ASTEP 400, as established from the point-to-point rms of the light curves after 3σ rejection of outlier points. Each point represents one light curve obtained over multiple consecutive nights. The long-time systematics have been taken into account in the light curve detrending. The red solid line represents a sixth-degree polynomial fit of the data points.

transit candidates. The BLS algorithm is also suitable for the detection of EcBs, as it searches for signals characterized by a periodic alternation between two discrete levels, with much less time spent at the lower level.

The BLS routine detected about 3000 candidates among the 310,000 observed stars brighter than $R = 17.5$ mag. Candidates with planet-transit-like features in their folded light curves were presented in Mékarnia et al. (2016). Most other candidates are bona fide EcBs, but the routine also detected intrinsic variable stars. Therefore, even if our approach was first focused on EcBs, we widen our study to all types of variable stars.

Based on figures showing plots of a complete light curve, a set of data covering a sequence of one to three days of observation, and the folded light curve using the period given by the BLS process (Figure 2), we rejected, as a first step, false or doubtful variation detections and filtered out light curves with low signal-to-noise ratios. The second step entailed determining the EcB or variable star type based on the period, the amplitude, the $B - V$ indices, and the shape of each light curve. In some cases we reanalyzed the data using Period04, a software package dedicated to period analysis (Lenz & Breger 2005), to achieve a more accurate classification. EcBs and other variables resulting from this study are presented in two separate catalogs.

3. THE ECLIPSING BINARIES CATALOG

Each BLS candidate was examined visually in order to detect a primary and a secondary minimum on the phased curve. The eventual variations between the levels of the two maximum were carefully examined to discriminate between activity and binarity.

For each star we give, in Table 2, the ASTEP and UCAC4 (Zacharias et al. 2013) identifications, the coordinates, the ASTEP red magnitude, the $B - V$ indices, the orbital period, the depth, the type of binary, EA (Algol type), EB (β Lyr type) or EW (W UMa type), and eventual comments. When only one minimum is seen in the data set, no period is given. The 3σ errors on the periods are computed with the formulae proposed by Montgomery & Odonoghue (1999). Eventual variability is mentioned in the comments. If the star was already known we note its name as given in the general catalog of variable stars (Kazarovets et al. 2009).

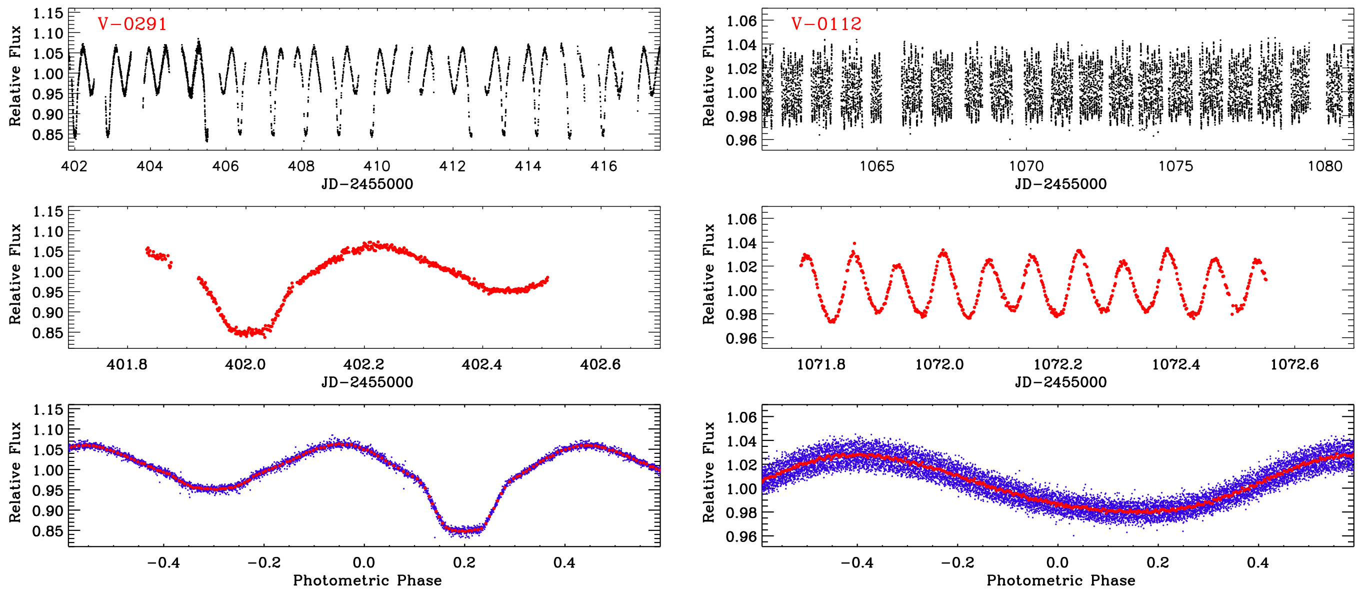

Figure 2. Two examples of figures used for the visual selection and characterization of EcBs (left) and variable stars (right). The figures present, from top to bottom, a complete light curve, a set covering one day of observation, and a phase-folded light curve.

Table 2
ASTEP 400 EcBs

Cat-ID	ASTEP-ID	UCAC4-ID	α (J2000)	δ (J2000)	R Mag	$B-V$	Period (day)	Error per. (day)	Depth	Type	Comments
V-0003	A-049-3024-0835	160-200841	$17^{h}33^{m}32.^{s}3$	$-58°09'49.''5$	10.73	0.31	0.86505	$7.7\ 10^{-6}$	0.49	EB	FU Ara
V-0009	A-012-0882-3469	120-133647	$15^{h}59^{m}12.^{s}7$	$-66°03'24.''2$	11.05	0.31	2.2813	$1.5\ 10^{-3}$	0.003	EB	⋯
V-0013	A-045-2416-3712	186-189607	$17^{h}34^{m}41.^{s}5$	$-52°55'23.''9$	11.11	0.41	1.3431	$2.1\ 10^{-4}$	0.037	EA	⋯
V-0029	A-030-0070-1137	117-116038	$15^{h}48^{m}59.^{s}2$	$-66°44'29.''2$	11.33	0.47	0.61462	$5.1\ 10^{-5}$	0.24	EA	GN Tra
V-0033	A-020-2322-2941	122-141723	$15^{h}54^{m}07.^{s}4$	$-65°40'03.''0$	11.37	−0.06	1.7784	$8.6\ 10^{-5}$	0.033	EW	⋯
V-0036	A-054-1290-1169	208-142270	$17^{h}08^{m}44.^{s}6$	$-48°28'32.''0$	11.39	0.73	⋯	⋯	0.045	EA	⋯
V-0053	A-044-2002-1787	160-202847	$17^{h}44^{m}14.^{s}2$	$-58°04'26.''0$	11.56	0.91	3.7593	$5.3\ 10^{-2}$	0.002	EW	⋯
V-0058	A-021-2504-3216	128-142859	$15^{h}45^{m}06.^{s}2$	$-64°35'18.''0$	11.59	0.43	8.1900	$1.3\ 10^{-1}$	0.002	EA	⋯
V-0066	A-044-0314-2596	161-203316	$17^{h}47^{m}28.^{s}8$	$-57°51'39.''2$	11.65	0.51	0.49212	$7.2\ 10^{-5}$	0.029	EB	⋯
V-0080	A-012-1206-3696	121-141548	$15^{h}58^{m}23.^{s}2$	$-65°59'58.''8$	11.75	−0.04	5.3186	$4.3\ 10^{-5}$	0.036	EA	⋯
V-0089	A-012-1830-1833	118-127053	$15^{h}56^{m}50.^{s}7$	$-66°28'42.''4$	11.79	0.90	2.9824	$3.5\ 10^{-4}$	0.026	EA	⋯
V-0144	A-052-3289-2419	186-184316	$17^{h}18^{m}48.^{s}0$	$-52°52'43.''3$	12.08	0.38	0.57897	$1.0\ 10^{-5}$	0.20	EB	⋯

Note. The complete table is available from CDS.

(This table is available in its entirety in machine-readable form.)

4. THE VARIABLE STARS CATALOG

Once the EcBs were classified, we examined the other stars detected by the BLS algorithm. We used the same type of figures (Figure 2) we used for EcBs to perform a visual inspection of each variable. Periods and amplitudes were computed with Period04. The main period and amplitude (semi-amplitude) of each star are given in the catalog (Table 3). The 3σ errors on the periods were computed with the formulae proposed by Montgomery & Odonoghue (1999). We did not calculate individual errors on the amplitudes, as they have no meaning for observations carried out with a large non-calibrated spectral band. In addition, for multi-periodic or asymmetric variables, the amplitude of the main period would change if we perform a complete period analysis. However, the mean error on the amplitude is estimated to one or two per thousand.

We detected 76 pure δ Scuti stars, 36 pure γ Doradus stars, and 13 hybrid γ Dor $-\delta$ Sct stars. The high-amplitude δ Scuti stars are denoted as HADS in the comments column. The γ Doradus stars with asymmetric light curves (large variations in the maximum brightness and much smaller variations in the minimum brightness) are noted Asym in the comments column. This phenomenon was first detected by Balona et al. (2011) in the *Kepler* stars. For the hybrids we give the period and amplitude of the first δ Sct and γ Dor mode in two separate rows. The 10 pulsating stars members of EcB systems are listed in specific tables (Tables 4 and 5). A classification as δ Sct and γ Dor is based on the value of the main period, the presence of multi-periodicity but also on the $B-V$ indices. If the $B-V$ indices are false some stars could actually be β Cepheid and SPB stars. Only one Cepheid was detected.

We detected 85 RR Lyrae stars. The sub-type (RRab, c, or d Lyr) and the eventual Blazhko effect are noted in the comments column. As the periods and light curve shapes of RRc Lyr stars are similar to those of other variable stars, we retain only stars showing the typical bump in the ascending curve. We found several stars with the same periods and curve shapes as RRab Lyr variables, but with much lower amplitudes. We think that they are bona fide RR Lyr type stars, but that

Table 3
ASTEP 400 Variables Stars

Cat-ID	ASTEP-ID	UCAC4-ID	α (J2000)	δ (J2000)	R Mag	$B - V$	Period (day)	Err. per. (day)	Amp.	Type	Comments
V-0001	A-049-1231-2340	162-191550	$17^h37^m00^s.1$	$-57°46'31''.6$	10.10	0.77	…	…	…	LPV	…
V-0002	A-049-1439-1529	161-201231	$17^h36^m36^s.9$	$-57°59'05''.4$	10.24	0.17	0.048076	$1.7\ 10^{-6}$	0.0033	δ Scuti	…
V-0004	A-049-1015-2984	162-191638	$17^h37^m24^s.1$	$-57°36'34''.5$	10.79	0.96	…	…	…	LPV	…
V-0005	A-049-1550-3825	164-188206	$17^h36^m21^s.6$	$-57°23'46''.6$	10.80	0.28	0.12950	$1.2\ 10^{-5}$	0.0033	δ Scuti	…
V-0006	A-030-1792-2547	119-123506	$15^h44^m30^s.5$	$-66°23'16''.1$	10.88	0.36	0.13493	$4.8\ 10^{-5}$	0.0060	δ Scuti	…
V-0007	A-037-2775-3230	175-187731	$17^h15^m13^s.0$	$-55°11'41''.9$	10.93	0.26	…	…	…	LPV	…
V-0008	A-030-0259-1680	117-115940	$15^h48^m28^s.5$	$-66°36'15''.4$	10.93	0.36	0.053305	$1.7\ 10^{-5}$	0.0026	δ Scuti	…
V-0010	A-030-2436-0282	116-116421	$15^h42^m52^s.0$	$-66°58'10''.6$	11.08	0.32	0.057176	$1.6\ 10^{-5}$	0.0032	δ Scuti	…
V-0011	A-030-0816-3507	120-130747	$15^h46^m57^s.2$	$-66°08'23''.0$	11.09	0.28	0.11364	$1.4\ 10^{-4}$	0.0015	Hybrid	(δ Sct)
	…	…	…	…	…	…	1.5067	$7.0\ 10^{-3}$	0.0053	Hybrid	(γ Dor)
V-0012	A-049-0774-0277	159-195536	$17^h37^m55^s.1$	$-58°18'06''.8$	11.10	1.45	…	…	…	LPV	…

Note. The complete table is available from CDS.

(This table is available in its entirety in machine-readable form.)

Table 4
List of ASTEP 400 Pulsating EcBs

Cat-ID	ASTEP-ID	UCAC4-ID	α (J2000)	δ (J2000)	R Mag	$B-V$	EB Type	Puls. type	Comments
V-0169	A-009-3162-3150	223-043030	$09^h51^m51\overset{s}{.}9$	$-45°26'01''.9$	12.19	0.18	EW	Hybrid	⋯
V-0258	A-020-3463-3598	123-150579	$15^h51^m18\overset{s}{.}8$	$-65°30'00''.3$	12.50	1.75	EW	δ Sct	⋯
V-0369	A-055-1555-0254	205-119768	$16^h23^m57\overset{s}{.}7$	$-49°06'07''.8$	12.89	0.13	EA	γ Dor	⋯
V-0757	A-012-0423-2567	119-127185	$16^h00^m25\overset{s}{.}0$	$-66°17'07''.6$	14.22	0.31	EB	δ Sct	⋯
V-0815	A-037-1281-3040	174-181249	$17^h17^m54\overset{s}{.}7$	$-55°14'26''.9$	14.38	−0.19	EA	δ Sct	IS Ara
V-0901	A-021-0355-2870	127-144405	$15^h50^m14\overset{s}{.}8$	$-64°40'23''.6$	14.64	⋯	EA	δ Sct	HADS
V-1045	A-055-3455-1140	206-116997	$16^h20^m59\overset{s}{.}4$	$-48°52'35''.0$	15.03	0.85	EA	δ Sct	⋯
V-1228	A-055-1724-2218	208-122066	$16^h23^m41\overset{s}{.}1$	$-48°35'56''.9$	15.54	0.14	EA	γ Dor	⋯
V-1276	A-055-2256-3723	209-116763	$16^h22^m50\overset{s}{.}9$	$-48°12'51''.6$	15.64	0.66	EB	δ Sct	⋯
V-1451	A-012-1295-2116	118-127346	$15^h58^m13\overset{s}{.}0$	$-66°24'16''.0$	16.04	⋯	EA	Hybrid	HADS

Table 5
Characteristics of ASTEP 400 Pulsating EcBs

Cat-ID	Eclipse			δ Sct			γ Dor		
	Period (day)	Error per. (day)	Depth	Period (day)	Error per. (day)	Amp.	Period (day)	Error per. (day)	Amp.
V-0169	1.8070	$4.3\ 10^{-3}$	0.001	0.079100	$6.7\ 10^{-6}$	0.0016	0.80879	$4.3\ 10^{-4}$	0.0026
V-0258	0.75518	$7.9\ 10^{-6}$	0.044	0.031893	$1.3\ 10^{-7}$	0.0044	⋯	⋯	⋯
V-0369	11.859	$7.1\ 10^{-2}$	0.026	⋯	⋯	⋯	2.4240	$3.5\ 10^{-2}$	0.0022
V-0757	3.5697	$1.3\ 10^{-4}$	0.120	0.041428	$3.5\ 10^{-7}$	0.0063	⋯	⋯	⋯
V-0815	1.6688	$4.4\ 10^{-6}$	0.430	0.043850	$1.0\ 10^{-6}$	0.0126	⋯	⋯	⋯
V-0901	⋯	⋯	0.170	0.058990	$3.4\ 10^{-7}$	0.0948	⋯	⋯	⋯
V-1045	⋯	⋯	0.150	0.15874	$9.1\ 10^{-5}$	0.0102	⋯	⋯	⋯
V-1228	10.451	$7.1\ 10^{-2}$	0.080	⋯	⋯	⋯	0.86070	$7.2\ 10^{-3}$	0.0054
V-1276	2.8189	$8.7\ 10^{-3}$	0.050	0.11801	$1.2\ 10^{-4}$	0.0060	⋯	⋯	⋯
V-1451	0.28160	$5.2\ 10^{-7}$	0.580	0.13536	$5.5\ 10^{-7}$	0.1271	3.5051	$4.9\ 10^{-4}$	0.0961

their observed amplitudes are reduced by the presence in the same or a nearby pixel of one or several brighter stars. In this case the identification given in Table 3 actually corresponds to the brightest nearby star and not to the hidden RR Lyr variable. We can only assert that a faint RR Lyr variable is present within 2 arcsec from the position given in the catalog.

We detected 609 stars with periods longer than the observation session. They are mainly red stars of diverse types (Mira, semi-regular pulsating stars, irregular variables, etc.). They are noted as long period variables (LPV) in the catalog. Because we observed only a portion of the variation cycle, we provide neither period nor amplitude for these stars.

The 93 stars presenting variations related to activity (spots, moving bumps, etc.) were classified as rotationally variable stars and noted Rot.V. The given period corresponds to the rotational period.

Finally, when we had some doubt about the classification of a star we noted it simply as variable. Two hundred fifty-three stars were classified as variables. The uncertainty could be due to the low signal-to-noise ratio of the faintest stars or be due to a very short observation session. When we hesitated between two particular classifications, such as between a W UMa EcB type and stellar activity or between a γ Dor type and stellar activity, we noted the star simply as variable in order to avoid false classifications.

5. CONCLUSIONS

We have provided a catalog of southern EcBs and variable stars using the photometric database of ASTEP 400, a semi-robotic telescope that is operated from Dome C in Antarctica, and whose main goal is to detect transiting exoplanets. Eighteen stellar fields (with a FOV of $1° \times 1°$) were observed during the 2010–2012 polar winter seasons, with two fields observed during two winter seasons. The typical photometric accuracy ranges from ~2 ppt for the brightest stars ($R \sim 12$ mag), with an integration time of 130 s, to ~20 ppt for the faintest stars ($R = 17$ mag).

The star classification was based on the period, using the period analysis software Period04, the amplitude, the $B - V$ indices, and the light curve shape. Our catalogs contain 673 EcBs and 1166 variable stars, among which 85 are RR Lyrae stars, 76 are pure δ Scuti stars, 36 are pure γ Doradus stars, 13 are hybrid γ Dor − δ Sct stars, 1 is a Cepheid, 93 stars present variations related to activity, and 609 are LPVs. Finally, 253 variables were not classified, as the duration of observations did not allow the determination of their types.

All the variables of our catalogs are the result of BLS detection. It is evident that BLS, which is well adapted for detecting EcBs, causes a bias in the detection of some types of variables. It is quite likely that a fraction of variables with complex shapes have not been detected. However, the BLS has enabled us to detect a wide range of variables. This leads us to believe that the bias induced by the BLS detection should not be as significant as expected. The detection of only one Cepheid is surprising but is probably related to the duration of observation rather than to the use of the BLS.

Due to our limited sample we did not use any automatic method either to perform variable false positive exclusion or for star classification. Even if the visual false positive exclusion was fast and easy to perform, the variable type classification required significant time. Consequently, automatic methods of detection and classification cannot be avoided for current and upcoming large surveys. Automated variable classification methods use machine-learning algorithms and generally have a low overall error rate (e.g., Drake et al. 2014; Paegert et al. 2014; Kim & Bailer-Jones 2016). In most cases, the selecting variable process is based on values of the Stetson variability index (Stetson 1996). However, the result of any automated classification is strongly linked with the ability to obtain a complete training data set, particularly in the early stages of a survey. These methods are particularly efficient for large amplitude asymmetric variables such as RR Lyrae stars, but the error rate may be quite high for some variable types such as γ Doradus. If automatic methods are well-suited for statistical studies on large surveys, individual analysis of each light curve, when the sample size allows it, remains necessary to get the most accurate possible classification.

All catalog light curves are available online via the ASTEP database[3] for the users who want to study specifically some of these stars.

The ASTEP project benefited from the support of the Agence Nationale de la Recherche, the Institut des Sciences de l'Univers, and the Programme National de Planétologie. We are indebted to the constant logistical support of the Institut polaire français Paul-Emile Victor (IPEV) and the Programma Nazionale di Ricerche in Antartide (PNRA), without which this project would not have been possible. We also wish to thank F. Valbousquet for his support in the development of the instrument, E. Bondoux for his valuable technical assistance, the Concordia winter-over DC6 and DC7 crews for their continuous and timely support, and G. Bouchez for his contribution during the winter-over in 2012. We wish to thank the anonymous referee for insightful comments that improved the clarity of the paper.

Software: OIS (Miller et al. 2008), BLS (Kovács et al. 2002), Period04 (Lenz & Breger 2005).

REFERENCES

Abe, L., Gonçalves, I., Agabi, A., et al. 2013, A&A, 553, A49
Andersen, M. I., Freyhammer, L., & Storm, J. 1995, in European Southern Observatory Conf. and Workshop Proc. 53, Calibrating and Understanding HST and ESO Instruments, ed. P. Benvenuti, 87
Baglin, A., Auvergne, M., Barge, P., et al. 2006, in ESA Special Publication 1306, The CoRoT Mission Pre-Launch Status—Stellar Seismology and Planet Finding, ed. M. Fridlund et al. (Noordwijk: ESA), 33
Balona, L. A., Guzik, J. A., Uytterhoeven, K., et al. 2011, MNRAS, 415, 3531
Borucki, W. J., Koch, D., Basri, G., et al. 2010, Sci, 327, 977
Daban, J.-B., Gouvret, C., Guillot, T., et al. 2010, Proc. SPIE, 7733, 4
Drake, A. J., Graham, M. J., Djorgovski, S. G., et al. 2014, ApJS, 213, 9
Kim, D.-W., & Bailer-Jones, C. A. L. 2016, A&A, 587, A18
Kovács, G., Zucker, S., & Mazeh, T. 2002, A&A, 391, 369
Lenz, P., & Breger, M. 2005, CoAst, 146, 53
Mékarnia, D., Guillot, T., Rivet, J.-P., et al. 2016, MNRAS, 463, 45
Miller, J. P., Pennypacker, C. R., & White, G. L. 2008, PASP, 120, 449
Montgomery, M. H., & Odonoghue, D. 1999, DSSN, 13, 28
Paegert, M., Stassun, K. G., & Burger, D. M. 2014, AJ, 148, 31
Kazarovets, E. V., Samus, N. N., Durlevich, O. V., et al. 2009, ARep, 53, 1013
Stetson, P. B. 1996, PASP, 108, 851
Walker, G., Matthews, J., Kuschnig, R., et al. 2003, PASP, 115, 1023
Zacharias, N., Finch, C. T., Girard, T. M., et al. 2013, AJ, 145, 44

[3] http://astep-vo.oca.eu